Coalescence of non-Markovian dissipation, quantum Zeno effect, and non-Hermitian physics in a simple realistic quantum system

G. Mouloudakis * and P. Lambropoulos
Department of Physics, University of Crete, P.O. Box 2208, 71003 Heraklion, Crete, Greece
and Institute of Electronic Structure and Laser, FORTH, P.O. Box 1527, 71110 Heraklion, Greece

(Received 28 June 2022; accepted 1 November 2022; published 14 November 2022)

Diagonalization of the effective Hamiltonian describing an open quantum system is the usual method of tracking its exceptional points (EPs). Although such a method is successful for tracking EPs in Markovian systems, it may be problematic in non-Markovian systems where a closed expression of the effective Hamiltonian describing the open system may not exist. In this work we provide an alternative method of tracking EPs in open quantum systems, using an experimentally measurable quantity, namely, the effective decay rate of a qubit. The quantum system under consideration consists of two nonidentical interacting qubits, one of which is coupled to an external environment. We develop a theoretical framework in terms of the time-dependent Schrödinger equations of motion, which provides analytical closed-form solutions of the Laplace transforms of the qubit amplitudes, enabling the study of various cases of environmental spectral densities. The link between the peaked structure of the effective decay rate of the qubit that interacts indirectly with the environment and the onset of the quantum Zeno effect is investigated, revealing the connections between the latter and the presence of exceptional points. Our treatment and results in addition reveal an intricate interplay between non-Markovian dynamics, the quantum Zeno effect, and non-Hermitian physics.

DOI: 10.1103/PhysRevA.106.053709

I. INTRODUCTION

The dissipative dynamics of open quantum systems coupled to non-Markovian reservoirs is a multifaceted field of fundamental as well as practical importance [1,2]. It pertains to a broad class of problems, ranging from quantum information processing to nonequilibrium statistical mechanics. The effective Hamiltonian describing an open quantum system is by necessity non-Hermitian, which brings up its possible connection with non-Hermitian physics [3], exceptional points [4], and related questions, in a field of wide-ranging interest and activity. In both of those fields and from different angles, the quantum Zeno effect (QZE) has been found to be a major participant. Having initially entered physics as a curiosity, it has been found to play an uncanny role in the protection against dissipation [5,6]. Although research in each one of the above three field has been active for many years, the synergy of phenomena related to those fields does not seem to have been noticed, let alone explored. Our recent work [7] on quantum dissipation in non-Markovian environments has steered us to a type of problem in which that synergy has been found to be astonishingly revelatory. The treatment of that problem and its consequences is the purpose of the present article. Before embarking on the discussion of formulation, computation, and results, we need to provide a brief outline of the background and past activity in each of the above three fields.

Dissipation is essentially inevitable in any process involving a quantum system, arising from its interaction with the environment, referred to as a reservoir, or even a class thereof. Note that the terms environment, reservoir, and bath are used interchangeably in the literature. A reservoir is characterized by a specific spectral density. Depending on whether that spectral density is smooth or exhibits a peaked behavior, at least in a range of energies encompassing the energy of the system, the reservoir is usually referred to as Markovian or non-Markovian, respectively. Physically speaking, the term Markovian refers to reservoirs for which the Markov approximation is valid. This implies that any excitation transferred from the system to the reservoir is irreversible, i.e., practically lost forever [8]. On the other hand, for non-Markovian reservoirs, although eventual loss is also present, the excitation may be transferred back to the system [9]. This exchange of excitation between system and reservoir lasts for finite times, whose length depends on the spectral density of the latter. The length of that time does in fact characterize the so-called Markovianity of the particular reservoir [1].

Although the interaction of a quantum system with an external environment does ultimately lead to dissipation, there is an important effect which, depending on the relative parameters of the compound system, may lead to protection against such types of dissipation. That effect, known as the quantum Zeno effect, reflects the possibility of the environment to freeze the dynamics of the quantum system or some part of it [5]. The QZE, the regions of its onset, and its implications have been studied in many different contexts such as in circuit-QED systems [10], ultracold atoms [11], and one-dimensional hybrid quantum circuit models [12], while many experiments have confirmed the possibility of freezing the evolution of the quantum state via such a mechanism [5,13–18].

*gmouloudakis@physics.uoc.gr

A number of studies have also pointed out the potential role of the QZE in the protection of quantum information between correlated qubits [19–22]. The results suggest that repeated projective measurements on a system of entangled qubits can lead to the preservation of entanglement, independently of the state in which the system is initially encoded. This effect appears when the state of the system evolves in a multidimensional subspace, usually referred to as the Zeno subspace [23,24]. Although fast repeated projective measurements directly on the system may freeze its evolution, this method may be somewhat restrictive for the implementation of quantum information processing tasks, where additional operations on the system may be necessary. An alternative approach relies on indirect measurements, where the apparatus does not act directly on the system, but detects a signal mediated by some field with which it interacts [25]. That work has however given rise to serious reservations as to the possibility of the occurrence of the QZE in such configurations [26–30]. On the other hand, it has been demonstrated that the QZE does not necessarily require projective measurements, as it may also be induced through continuous strong couplings [18,31–34].

In recent work [35] Wu and Lin investigated the QZE in dissipative systems beyond the Markov, rotating-wave, and perturbative approximations, in the context of a spin-boson model, which describes the interaction between a spin system and a bosonic bath. Their study suggested that the non-Markovian character of the bath may be favorable for the accessibility of the QZE in such systems, as it may prolong the quantum Zeno time and lead to multiple Zeno–anti-Zeno crossover phenomena.

At the same time, the transitions to the quantum Zeno regime have been recently shown to be linked with the parity-time ($\mathcal{PT}$)-symmetry breaking of the non-Hermitian Hamiltonian which describes the open quantum system [36–40]. The boundary between the unbroken and broken $\mathcal{PT}$ symmetry of a Hamiltonian describing an open quantum system [41,42] is marked by the presence of exceptional points (EPs) [43–46] where two or more eigenvalues coalesce while their corresponding eigenvectors become parallel. It has also been demonstrated that the onset of the QZE is marked by a cascade of transitions in the system dynamics, as the strength of a continuous partial measurement on the open system is increased [47].

Tracking of EPs in open quantum systems is of crucial importance, since the system appears to exhibit enhanced sensitivity in their vicinity [48–50]. For Nth-order EPs, i.e., EPs that mark the coalescence of N eigenvalues, the sensitivity in the response of the system to small perturbations in parameter space has been confirmed to become more pronounced as N is increased [50–52].

Although in open Markovian systems, tracking EPs through diagonalization of the corresponding effective Hamiltonian is a rather easy theoretical task, that method is rather problematic in non-Markovian systems, for which it may not even be possible to construct an effective Hamiltonian describing the open system. In that case, alternative methods capable of tracking EPs indirectly, without the need of finding the eigenvalues of the open system, should be sought.

In this work we develop such a method, illustrating its advantage in a simple open quantum system consisting of two interacting qubits, one of which is coupled to an external environment. Our formulation allows for the derivation of analytical expressions of the Laplace transforms of the qubit amplitudes, enabling the study of the effects of various types of reservoir spectral densities on the system. If the qubit not directly coupled to the environment is initially in its excited state, then as the coupling between the remaining qubit and the environment increases, we observe a phase transition to the Zeno regime, resulting in increased protection against the population dissipation that the environment inevitably induces. A glimpse of this effect was reported recently in an recent paper of ours, for a system of XX spin chains boundary driven by non-Markovian environments, where the total population of the chain was found to become increasingly protected against dissipation, for sufficiently large boundary couplings [7]. Here we investigate the connection between these types of phase transitions and the presence of exceptional points for both Markovian and non-Markovian environments, using an experimentally measurable quantity, namely, the effective decay rate of the qubit that does not communicate directly with the reservoir. Based on a comparative analysis with the case of a Markovian reservoir, for which the system is diagonalizable, we argue that the effective decay rate may be used as a method for tracking the onset of the QZE in an non-Markovian open quantum system, as well as its EPs.

The rest of the paper is organized as follows. In Sec. II we outline the theoretical formulation of the problem, in the case of two nonidentical interacting qubits, one of which is coupled to an external environment characterized by an arbitrary spectral density. In Sec. III we provide the results of our study as well as a discussion related to the effects associated with the onset of QZE in the population dynamics of the qubits and its link to exceptional points. In Sec. IV we provide a summary of the results, with concluding remarks and an outlook for further inquiry.

II. THEORY

Our system consists of two nonidentical qubits and an environment characterized by a specific spectral density $J(\omega)$. The two qubits are interacting with a coupling strength $\mathcal{J}$ while the environment is interacting with the second qubit with a coupling strength g. Without loss of generality, we assume that the coupling strengths $\mathcal{J}$ and g are real numbers. A schematic representation of our system is depicted in Fig. 1.

The Hamiltonian of our system $\hat{\mathcal{H}} = \hat{\mathcal{H}}_S + \hat{\mathcal{H}}_E + \hat{\mathcal{H}}_I$ consists of three parts, namely, the Hamiltonian $\hat{\mathcal{H}}_S$, which describes our system of qubits and their mutual interaction, the Hamiltonian of the bosonic environment $\hat{\mathcal{H}}_E$, and the interaction Hamiltonian $\hat{\mathcal{H}}_I$, which describes the interaction between the second qubit and the environment. These three Hamiltonian terms are given by the expressions ($\hbar = 1$)

$$\hat{\mathcal{H}}_S = \omega_g |g\rangle_1\,{}_1\langle g| + \omega_e |e\rangle_1\,{}_1\langle e| + \omega_g' |g\rangle_2\,{}_2\langle g| + \omega_e' |e\rangle_2\,{}_2\langle e| + \mathcal{J}(\hat{\sigma}_1^+\hat{\sigma}_2^- + \hat{\sigma}_1^-\hat{\sigma}_2^+), \tag{1a}$$

$$\hat{\mathcal{H}}_E = \sum_\lambda \omega_\lambda \hat{a}_\lambda^{E\dagger}\hat{a}_\lambda^E, \tag{1b}$$

$$\hat{\mathcal{H}}_I = \sum_\lambda g(\omega_\lambda)\left(\hat{a}_\lambda^E\hat{\sigma}_2^+ + \hat{a}_\lambda^{E\dagger}\hat{\sigma}_2^-\right), \tag{1c}$$

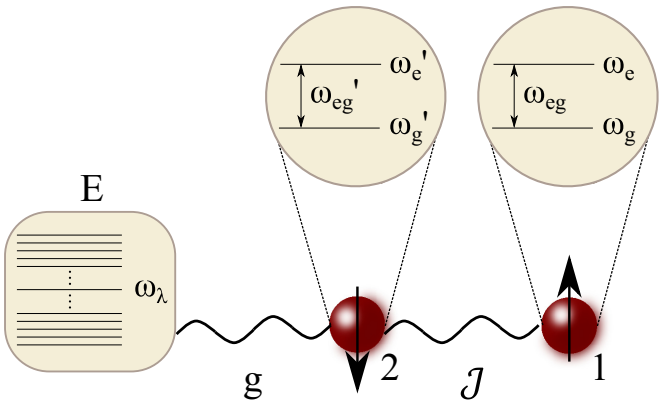

FIG. 1. Schematic representation of the system under study. Two nonidentical qubits are interacting with a coupling strength $\mathcal{J}$, while one of them is also coupled to an external environment E via a coupling g.

where ω_g and ω_e are the energies of the ground and excited states of the first qubit, respectively, ω'_g and ω'_e are the energies of the ground and excited states of the second qubit, respectively, ω_λ is the energy of the λth mode of the environment, $\hat{\sigma}_j^+ = |e\rangle_{j\,j}\langle g|$ and $\hat{\sigma}_j^- = |g\rangle_{j\,j}\langle e|$ $(j = 1, 2)$ are the qubit raising and lowering operators, respectively, and $\hat{a}_\lambda^E$ and $\hat{a}_\lambda^{E\dagger}$ are the quantum annihilation and creation operators of the environment, respectively.

The wave function of the whole system in the single-excitation space can be expressed as

$$|\Psi(t)\rangle = c_1(t)|\psi_1\rangle + c_2(t)|\psi_2\rangle + \sum_\lambda c_\lambda^E(t)\big|\psi_\lambda^E\big\rangle, \tag{2}$$

where

$$|\psi_1\rangle = |e\rangle_1|g\rangle_2|0\rangle_E, \tag{3a}$$
$$|\psi_2\rangle = |g\rangle_1|e\rangle_2|0\rangle_E, \tag{3b}$$
$$|\psi_\lambda^E\rangle = |g\rangle_1|g\rangle_2|00\ldots01_\lambda0\ldots00\rangle_E. \tag{3c}$$

By adopting the transformations for the qubit and environment amplitudes, namely, $c_1(t) = e^{-i(\omega'_g+\omega_e)t}\tilde{c}_1(t)$, $c_2(t) = e^{-i(\omega_g+\omega'_e)t}\tilde{c}_2(t)$, and $c_\lambda^E(t) = e^{-i(\omega_g+\omega'_g+\omega_\lambda)t}\tilde{c}_\lambda^E(t)$, it is easy to show that the time-dependent Schrödinger equation leads to the equations of motion of the amplitudes marked with a tilde

$$\frac{d\tilde{c}_1(t)}{dt} = -i\mathcal{J}\tilde{c}_2(t)e^{-i\varepsilon t}, \tag{4a}$$
$$\frac{d\tilde{c}_2(t)}{dt} = -i\mathcal{J}\tilde{c}_1(t)e^{+i\varepsilon t} - i\sum_\lambda g(\omega_\lambda)e^{-i\Delta_\lambda t}\tilde{c}_\lambda^E(t), \tag{4b}$$
$$\frac{d\tilde{c}_\lambda^E(t)}{dt} = -ig(\omega_\lambda)e^{+i\Delta_\lambda t}\tilde{c}_2(t), \tag{4c}$$

where $\varepsilon \equiv (\omega'_e - \omega'_g) - (\omega_e - \omega_g) \equiv \omega'_{eg} - \omega_{eg}$ is the difference between the two qubit energies and $\Delta_\lambda \equiv \omega_\lambda - (\omega'_e - \omega'_g) \equiv \omega_\lambda - \omega'_{eg}$ is the detuning between the energy of the λth mode of the environment and the excitation energy of the second qubit.

Formal integration of Eq. (4c) under the initial condition $\tilde{c}_\lambda^E(0) = 0$ [which is equivalent to $c_\lambda^E(0) = 0$] and substitution back into Eq. (4b) yields

$$\frac{d\tilde{c}_2(t)}{dt} = -i\mathcal{J}\tilde{c}_1(t)e^{+i\varepsilon t} - \int_0^t \sum_\lambda [g(\omega_\lambda)]^2 e^{-i\Delta_\lambda(t-t')}\tilde{c}_2(t')dt'. \tag{5}$$

At this point we replace the sum over all the modes of the environment by a frequency integral, according to the relation $\sum_\lambda [g(\omega_\lambda)]^2 \to \int d\omega J(\omega)$, where $J(\omega)$ is the spectral density of the environment. In view of this substitution, Eq. (5) becomes

$$\frac{d\tilde{c}_2(t)}{dt} = -i\mathcal{J}\tilde{c}_1(t)e^{+i\varepsilon t} - \int_0^t R(t-t')\tilde{c}_2(t')dt', \tag{6}$$

where $R(t)$ is defined via

$$R(t) \equiv \int_0^\infty J(\omega)e^{-i\Delta t}d\omega, \tag{7}$$

with $\Delta = \omega - \omega'_{eg}$. Equations (4a) and (6) now form our set of differential equations we wish to solve for $\tilde{c}_1(t)$. Taking the Laplace transform of these equations and using the Laplace transform properties of frequency shifting and convolution, we readily obtain

$$sF_1(s) = c_1(0) - i\mathcal{J}F_2(s + i\varepsilon), \tag{8a}$$
$$sF_2(s) = c_2(0) - i\mathcal{J}F_1(s - i\varepsilon) - B(s)F_2(s), \tag{8b}$$

where $F_1(s)$ and $F_2(s)$ are the Laplace transforms of the amplitudes marked by a tilde $\tilde{c}_1(t)$ and $\tilde{c}_2(t)$, respectively, while $B(s)$ is the Laplace transform of $R(t)$. Note that we also use the fact that the amplitudes marked by a tilde are equal to the amplitudes at $t = 0$. Although the above set of equations can be solved for $F_1(s)$ and $F_2(s)$ for arbitrary initial conditions, for the purposes of our study we focus on the expression of $F_1(s)$ for initial excitation on the first qubit, i.e., $c_1(0) = 1$ and $c_2(0) = 0$. In that case, we can easily show that $F_1(s)$ is given by the expression

$$F_1(s) = \frac{1}{s + \frac{\mathcal{J}^2}{s+i\varepsilon+B(s+i\varepsilon)}}. \tag{9}$$

Before proceeding with the calculation of the inversion integral, to obtain the time dependence of $\tilde{c}_1(t)$, we need to specify the spectral density function of the environment so that we can derive $R(t)$ according to Eq. (7) and hence the expression of its Laplace transform $B(s)$. Special cases of environments with Markovian, Lorentzian, or Ohmic spectral densities are studied in great detail in Sec. III, revealing the regions of parameters that affect the onset of the quantum Zeno regime.

It is important to note that our formalism can be used to explore much more complex systems, involving an arbitrary number of qubits and/or environments. A rather interesting result arises if we consider a system in which qubit 1 of Fig. 1 does not interact directly with only one qubit (qubit 2) but with an arbitrary number of qubits N, each one of which is coupled to its own environment. Using our formulation, we can show that, if all of the qubits are identical and the surrounding environments are characterized by the same spectral density,

the Laplace transform of the amplitude marked by a tilde of the first qubit is given by

$$F_1(s) = \frac{1}{s + \frac{N\mathcal{J}^2}{s+B(s)}}. \tag{10}$$

This equation is essentially the same as Eq. (9) for $\varepsilon = 0$ (identical qubits), with the exception of a factor of N multiplying $\mathcal{J}^2$, where N is the number of qubits interacting with qubit 1. In other words, the system consisting of a qubit (qubit 1) interacting with N qubits that communicate with N respective environments with identical spectral densities can be effectively considered equivalent to a two-qubit plus one-environment system (Fig. 1) with a collective coupling $\sqrt{N}\mathcal{J}$ between the two qubits. On the other hand, if all of the N qubits that interact with qubit 1 are communicating with a common environment, it is straightforward to show that $F_1(s)$ acquires the form

$$F_1(s) = \frac{1}{s + \frac{N\mathcal{J}^2}{s+NB(s)}}, \tag{11}$$

where the factor of N now multiplies both $\mathcal{J}^2$ and $B(s)$.

III. RESULTS AND DISCUSSION

A. Markovian reservoir

The coupling of a system to a reservoir within the Born (weak-coupling) approximation is Markovian if in addition the spectral density of the reservoir, as a function of energy, is smooth and slowly varying in the extended vicinity of the system transition energy. A formulation in terms of a Lindblad master equation for the time evolution of the reduced density operator of the system leads to a set of linear differential equations. In those equations the diagonal matrix elements involve damping coefficients proportional to the square of the constant coupling the system to the reservoir, whereas the off-diagonal matrix elements, in the absence of other dephasing interactions, involve damping constants one-half of that for the respective diagonal matrix element [53]. In fact, in an N-level ladder system, the damping of an off-diagonal matrix element connecting two decaying levels is one-half of the sum of the respective diagonal damping constants. The spontaneous decay of an excited atomic state in open space and the loss of a cavity mode coupled to a bosonic reservoir are two well-known examples. In both cases, the reservoir is bosonic, representing the standard model for dissipation in a quantum system. The derivation and time evolution of the system reduced density operator are standard textbook material that can be found in any book on quantum optics [53,54] or quantum electrodynamics [55]. We nevertheless show below the master equation governing the time evolution of the reduced density operator ρ, in the interaction picture, of a two-level system coupled to a bosonic reservoir at zero temperature

$$\partial_t \rho = \tfrac{1}{2}\tilde{\gamma}(2\sigma_-\rho\sigma_+ - \sigma_+\sigma_-\rho - \rho\sigma_+\sigma_-), \tag{12}$$

where $\sigma_+ \equiv |e\rangle\langle g|$ and $\sigma_- \equiv |g\rangle\langle e|$ are the raising and lowering operators of the two-level system, respectively, with $|e\rangle$ and $|g\rangle$ the upper and lower states. The coefficient $\tilde{\gamma}$ is the resulting relaxation constant which, to within some coefficients depending on the particular physical system, is proportional to the square of the constant coupling the system to the reservoir. In addition to the damping, the derivation leads to a shift, which in our case is of no relevance.

In this paper we are dealing with two interacting qubits, one of which is coupled to reservoirs of various spectral densities. It can be viewed as a basic component of a chain of qubits, in which case the end qubits are often referred to as boundaries. Our system is generic in the sense that we do not assume any specific physical realization of the qubits. They could be quantum dots, two-level cold atoms, superconducting Josephson, etc. The results and predictions of our analysis would therefore be applicable to a chain of any physical qubit realization. The nature of the coupling constants entering our formulation would then depend on the realization. The general structure of the equations would however be the same. The relative magnitude of the coupling constants employed in our analysis merits a comment, as it is of significance. Viewing the two-qubit system as a basic component of a chain of a vehicle for information transfer [7], the parameter $\mathcal{J}$ is of controlling importance. It is for that reason that the magnitude of all other parameters is defined in relation to $\mathcal{J}$.

Although for a Markovian reservoir the dynamics are amenable to a description in terms of a master equation, for non-Markovian reservoirs such a formulation is not possible. Given our emphasis on non-Markovian cases, we have developed the formalism in terms of the amplitudes of the Schrödinger equation, described in the preceding section. From the solutions for the amplitudes, if needed, the corresponding expressions for the density matrix elements are readily constructed.

Returning to the Markovian case, using well-known results outlined above, all we need to do is add to the transition energy of the second qubit the imaginary part $-i\tilde{\gamma}/2$, where $\tilde{\gamma}$ is the decay rate of that qubit, due to the coupling to the Markovian reservoir. It bears repeating that $\tilde{\gamma}$ is proportional to the square of the coupling constant $g(\omega_\lambda)$, evaluated at the transition energy of the qubit, as dictated by the δ function in the identity $\lim_{\varepsilon\to 0^+}\frac{1}{x\pm i\varepsilon} = \mathbb{P}\frac{1}{x} \mp i\pi\delta(x)$ employed in the elimination of the degrees of freedom of the reservoir. There is nothing phenomenological about this procedure, in which well-known textbook rigorous results are invoked. Note that since $\varepsilon \equiv \omega'_{eg} - \omega_{eg}$, the decay term $-i\tilde{\gamma}/2$ in the transition energy of the second qubit is also transferred to ε. Making the substitution $\varepsilon \to \varepsilon - i\tilde{\gamma}/2$ in the expression of $F_1(s)$ for $B(s) = 0$ (the effects of the Markovian reservoir are taken into account through the substitution $\varepsilon \to \varepsilon - i\tilde{\gamma}/2$) in Eq. (9), we obtain

$$F_1(s) = \frac{s + (\tilde{\gamma}/2 + i\varepsilon)}{s^2 + (\tilde{\gamma}/2 + i\varepsilon)s + \mathcal{J}^2}. \tag{13}$$

The Laplace inversion of Eq. (13) provides the time evolution of the amplitude marked by a tilde of qubit 1. An insightful expression can be obtained in the case of identical qubits ($\varepsilon = 0$), where the Laplace inversion yields

$$\tilde{c}_1(t) = e^{-\tilde{\gamma}t/4}\left[\cos\left(\frac{t}{4}\sqrt{(4\mathcal{J})^2 - \tilde{\gamma}^2}\right) + \frac{\tilde{\gamma}}{\sqrt{(4\mathcal{J})^2 - \tilde{\gamma}^2}}\sin\left(\frac{t}{4}\sqrt{(4\mathcal{J})^2 - \tilde{\gamma}^2}\right)\right], \quad \tilde{\gamma} \neq 4\mathcal{J} \tag{14}$$

and $\tilde{c}_1(t) = e^{-\mathcal{J}t}(1+\mathcal{J}t)$ for $\tilde{\gamma} = 4\mathcal{J}$. It is interesting to observe that for $\tilde{\gamma} \ll 4\mathcal{J}$, the amplitude marked by a tilde of the first qubit follows an oscillatory behavior with frequency equal to $\frac{\sqrt{(4\mathcal{J})^2-\tilde{\gamma}^2}}{4}$ along with an exponential decay. As $\tilde{\gamma}$ approaches the value $4\mathcal{J}$ the oscillations tend to disappear, and when $\tilde{\gamma} = 4\mathcal{J}$ the oscillatory part $[\cos(\frac{t}{4}\sqrt{(4\mathcal{J})^2-\tilde{\gamma}^2}) + \frac{\tilde{\gamma}}{\sqrt{(4\mathcal{J})^2-\tilde{\gamma}^2}}\sin(\frac{t}{4}\sqrt{(4\mathcal{J})^2-\tilde{\gamma}^2})]$ reduces to a form which is linear in time, i.e., $(1+\mathcal{J}t)$. In the $\tilde{\gamma} \gg 4\mathcal{J}$ limit, using the identities $\cos(ix) = \cosh x$ and $\sin(ix) = i\sinh x$, it is straightforward to show that $\tilde{c}_1(t) \to 1$. Although this result may seem counterintuitive at first glance, it can be interpreted in terms of the QZE, i.e., a strong coupling between the second qubit and the Markovian environment causes the second qubit to freeze in its ground state, preventing qubit 1 from transferring population to qubit 2 and hence to the environment. Therefore, the population of the first qubit becomes protected against dissipation. Note that for this scheme to work, it is crucial not to have an initially populated second qubit, because in that case, the part of population of the second qubit would quickly dissipate due to the strong coupling between the latter and the environment.

Diagonalization of $\hat{\mathcal{H}}_S$ after the substitution $\omega_e' \to \omega_e' - i\tilde{\gamma}/2$ leads to the four eigenvalues

$$\lambda_1 = \omega_g + \omega_g', \tag{15a}$$

$$\lambda_2 = \omega_e + \omega_e' - \frac{i\tilde{\gamma}}{2}, \tag{15b}$$

$$\lambda_3 = \frac{1}{2}\left(\omega_g + \omega_g' + \omega_e + \omega_e' - \frac{i\tilde{\gamma}}{2}\right) - \frac{1}{4}\sqrt{(4\mathcal{J})^2 - (\tilde{\gamma}+2i\varepsilon)^2}, \tag{15c}$$

$$\lambda_4 = \frac{1}{2}\left(\omega_g + \omega_g' + \omega_e + \omega_e' - \frac{i\tilde{\gamma}}{2}\right) + \frac{1}{4}\sqrt{(4\mathcal{J})^2 - (\tilde{\gamma}+2i\varepsilon)^2}. \tag{15d}$$

Note that since we focus on the single-excitation subspace we only need to consider the eigenvalues λ_3 and λ_4. Equivalently, if we diagonalize $\hat{\mathcal{H}}_S$ in the single-excitation subspace, which would be essentially a 2×2 matrix, its eigenvalues are λ_3 and λ_4.

In Fig. 2(a) we plot the imaginary part of the eigenvalues λ_3 and λ_4 as a function of $\tilde{\gamma}$ for various values of the energy difference between the two qubits ε. As shown, in the case of identical qubits ($\varepsilon = 0$), the imaginary parts of the two eigenvalues coalesce at $\tilde{\gamma} = 4\mathcal{J}$ and they split for $\tilde{\gamma} > 4\mathcal{J}$. The point $\tilde{\gamma} = 4\mathcal{J}$ is called an exceptional point [43,44] and marks the boundary between the unbroken and the broken $\mathcal{PT}$ symmetry of the Hamiltonian. At the exceptional point, both the real and the imaginary parts of λ_3 and λ_4 coalesce, while the corresponding eigenvectors $|\phi_3\rangle$ and $|\phi_4\rangle$ given by the expressions below become parallel:

$$|\phi_3\rangle = |g\rangle_1|e\rangle_2 + \frac{1}{2\mathcal{J}}\left[-\left(\varepsilon - \frac{i\tilde{\gamma}}{2}\right) - \frac{1}{2}\sqrt{(4\mathcal{J})^2 - (\tilde{\gamma}+2i\varepsilon)^2}\right]|e\rangle_1|g\rangle_2, \tag{16a}$$

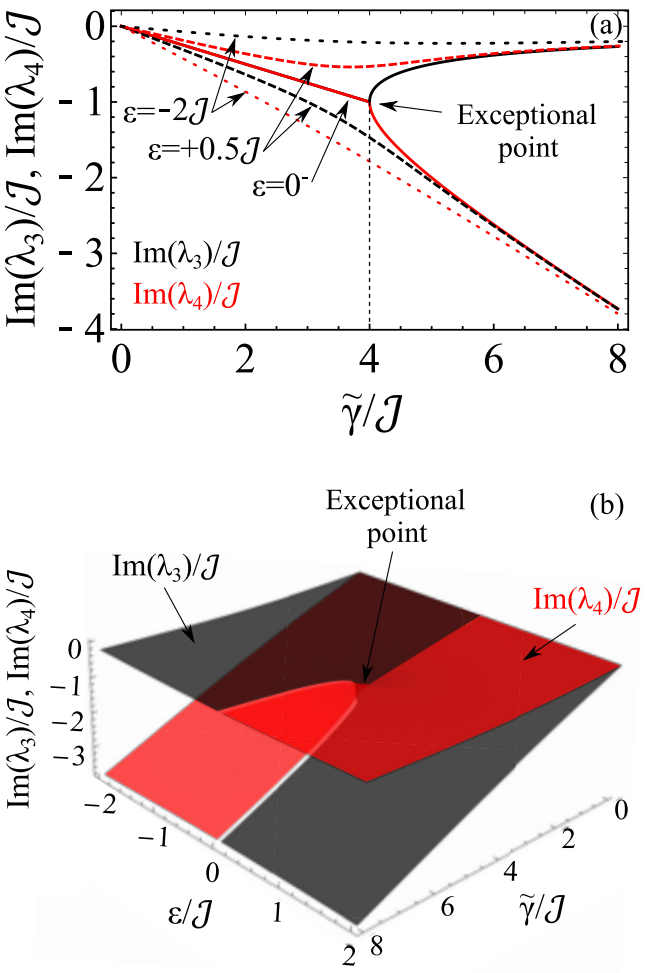

FIG. 2. (a) Imaginary parts of the eigenvalues λ_3 (black) and λ_4 (red) as a function of $\tilde{\gamma}$ for various values of the energy difference between the two qubits ε. The solid line denotes $\varepsilon = 0$, the dashed line $\varepsilon = -2\mathcal{J}$, and the dotted line $\varepsilon = 0.5\mathcal{J}$. The vertical dashed line indicates the position of the exceptional point for $\varepsilon = 0^-$, i.e., $\tilde{\gamma} = 4\mathcal{J}$. (b) Imaginary parts of the eigenvalues λ_3 (black) and λ_4 (red) on the ε-γ plane.

$$|\phi_4\rangle = |g\rangle_1|e\rangle_2 + \frac{1}{2\mathcal{J}}\left[-\left(\varepsilon - \frac{i\tilde{\gamma}}{2}\right) + \frac{1}{2}\sqrt{(4\mathcal{J})^2 - (\tilde{\gamma}+2i\varepsilon)^2}\right]|e\rangle_1|g\rangle_2. \tag{16b}$$

For $\varepsilon \neq 0$, the imaginary parts of λ_3 and λ_4 are different for any value of $\tilde{\gamma} \neq 0$ and therefore no exceptional point exists in that case. It is interesting to note that there is an abrupt interchange between the values of $\mathrm{Im}(\lambda_3)$ and $\mathrm{Im}(\lambda_4)$ as ε approaches zero. This behavior can be explained by visualizing these quantities in the ε-$\tilde{\gamma}$ plane, as shown in Fig. 2(b). This abrupt change is based on the complex eigenvalue topology of the involved intersecting Riemann sheets across the $\varepsilon = 0$ surface. The particular topology also suggests that the directionality of the motion in the ε-γ space, when encircling the exceptional point, with starting points on different Riemann sheets, plays an important role on the final outcome.

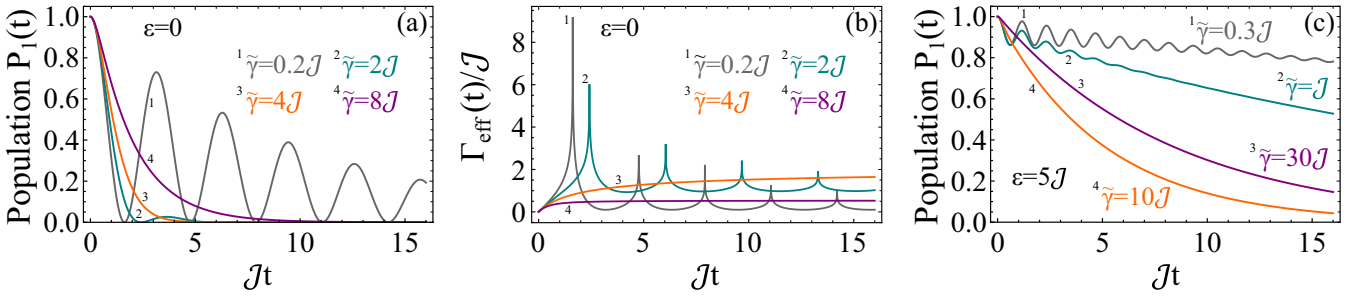

FIG. 3. (a) Population of qubit 1 in the configuration of Fig. 1, as a function of the time for various values of $\tilde{\gamma}$ and $\varepsilon = 0$. The gray line (labeled 1) denotes $\tilde{\gamma} = 0.2\mathcal{J}$, the teal line (2) $\tilde{\gamma} = 2\mathcal{J}$, the orange line (3) $\tilde{\gamma} = 4\mathcal{J}$, and the purple line (4) $\tilde{\gamma} = 8\mathcal{J}$. (b) Time dynamics of the effective decay Γ_{eff} using the same parameters as those in (a). (c) Population of qubit 1, as a function of time for various values of $\tilde{\gamma}$ and $\varepsilon = 5\mathcal{J}$. The gray lie (1) denotes $\tilde{\gamma} = 0.3\mathcal{J}$, the teal line (2) $\tilde{\gamma} = \mathcal{J}$, the orange line (3) $\tilde{\gamma} = 10\mathcal{J}$, and the purple line (4) $\tilde{\gamma} = 30\mathcal{J}$.

In Fig. 3(a) we show the time population dynamics of the first qubit of the configuration depicted in Fig. 1. The population dynamics is studied for various values of $\tilde{\gamma}$ and $\varepsilon = 0$ (identical qubits). For small values of $\tilde{\gamma}$ such that $\tilde{\gamma} \ll 4\mathcal{J}$ (gray line), the population exhibits damped oscillations indicative of the transfer of the excitation to the second qubit along with the environmental dissipation. As $\tilde{\gamma}$ is increased the oscillations become increasingly damped and less frequent (teal line), while at the critical coupling $\tilde{\gamma} = 4\mathcal{J}$ where the exceptional point lies, the oscillations disappear and the population dynamics is given by the expression $P_1(t) = e^{-2\mathcal{J}t}(1 + \mathcal{J}t)^2$ (orange line). For increasing values of $\tilde{\gamma}$ the population retains its nonoscillatory behavior and becomes increasingly protected against dissipation through the QZE (purple line). In the limit $\tilde{\gamma} \gg 4\mathcal{J}$, as also our analytical study suggests, the population of the first qubit remains essentially frozen in its initial value. Strictly speaking, complete freezing occurs in the limit of infinite $\tilde{\gamma}$, which is of only mathematical interest, as it is the range of finite but large values, in the sense of the above inequality, that are of realistic relevance. The same conclusions can be deduced by studying the effective decay rate of the probability $P_1(t)$, an important and widely used tool in the context of QZE in open quantum systems, defined as

$$\Gamma_{\text{eff}}(t) \equiv -\frac{1}{t}\ln[P_1(t)], \tag{17a}$$

which leads to

$$P_1(t) = e^{-\Gamma_{\text{eff}}(t)t}, \tag{17b}$$

indicating a decay rate with a time-dependent exponent.

In Fig. 3(b) we show the time dynamics of the effective decay rate $\Gamma_{\text{eff}}(t)$ using parameters identical to those of Fig. 3(a). Clearly, for $\tilde{\gamma} < 4\mathcal{J}$, the effective decay rate exhibits peaks associated with the population oscillations between the two qubits, whose frequency depends upon $\tilde{\gamma}$. The time between subsequent peaks increases as $\tilde{\gamma}$ is increased, while each subsequent peak is less pronounced compared to the preceding one. For $\tilde{\gamma} \geqslant 4\mathcal{J}$, the effective decay rate does not exhibit any peak and its value tends to decrease as $\tilde{\gamma}$ is increased.

However, the situation is quite different if the two qubits are nonidentical, as is the case in Fig. 3(c), where $\varepsilon = 5\mathcal{J}$. As Fig. 3(c) also suggests, we do not expect any qualitative transition on the system's response as $\tilde{\gamma}$ approaches and exceeds the value $\tilde{\gamma} = 4\mathcal{J}$. In this case, what determines the dissipation behavior is the ratio of ε to $\tilde{\gamma}$. In other words, as $\tilde{\gamma}$ is increased the dissipation of $P_1(t)$ is also increased, but if $\tilde{\gamma}$ becomes sufficiently larger than ε, the picture changes with the population of the first qubit becoming increasingly robust against dissipation. Again, even for $\varepsilon \neq 0$, in the limit where $\tilde{\gamma}$ is much larger than $\mathcal{J}$ and ε, the QZE freezes the dynamics of the second qubit, inducing thus a hindering of the decay of the first qubit population.

As is also evident from Fig. 3(b), in the long-time limit, the effective decay rate $\Gamma_{\text{eff}}(t)$ tends to stabilize to a finite nonzero value. The results of Fig. 3(c) become much clearer if we plot $\Gamma_{\text{eff}}(\tau)$ as a function of $\tilde{\gamma}$, where τ is defined to be a time much longer than any other timescale of the system. This quantity informs us about the onset of the QZE since it indicates the coupling $\tilde{\gamma}$ where the decay becomes maximum and decreases thereafter. As seen in Fig. 4(a), for $\varepsilon = 0$ and increasing $\tilde{\gamma}$, the decay is also increased until the point $\tilde{\gamma} = 4\mathcal{J}$, where it becomes a maximum. As $\tilde{\gamma}$ crosses the value $4\mathcal{J}$ there is an abrupt change in the behavior of the decay, as also suggested by Fig. 4(b), where we show the derivative of the effective decay rate with respect to $\tilde{\gamma}$. In view of the analysis of Fig. 2, the sharp peak at $\tilde{\gamma} = 4\mathcal{J}$ therefore indicates the position of the exceptional point.

On the other hand, for finite ε, i.e., nonidentical qubits, although the effective decay rate calculated at long times also exhibits a maximum, the curve around the maximum is smooth. In this case, according to Fig. 2, we should not expect any exceptional points at any coupling strength $\tilde{\gamma}$. For increasing ε, the decay rate as a function of $\tilde{\gamma}$ exhibits an increased width, which indicates that it takes a larger coupling window to cross the maximum and move from regions of increasing dissipation to the quantum Zeno regime, in compatibility with Fig. 3(c).

Our results suggest that the onset of the QZE is not necessarily associated with the presence of an exceptional point but with a peaked structure of the effective decay rate as a function of the coupling strength between the second qubit and the environment. The presence of an exceptional point, on the other hand, always indicates an abrupt phase transition from the anti-Zeno to the Zeno regime and is associated with a sharp peak of the effective decay rate as a function of $\tilde{\gamma}$. The link between these sharp peaks and the presence of EPs was also pointed out in a recent paper by Kumar *et al.* [37].

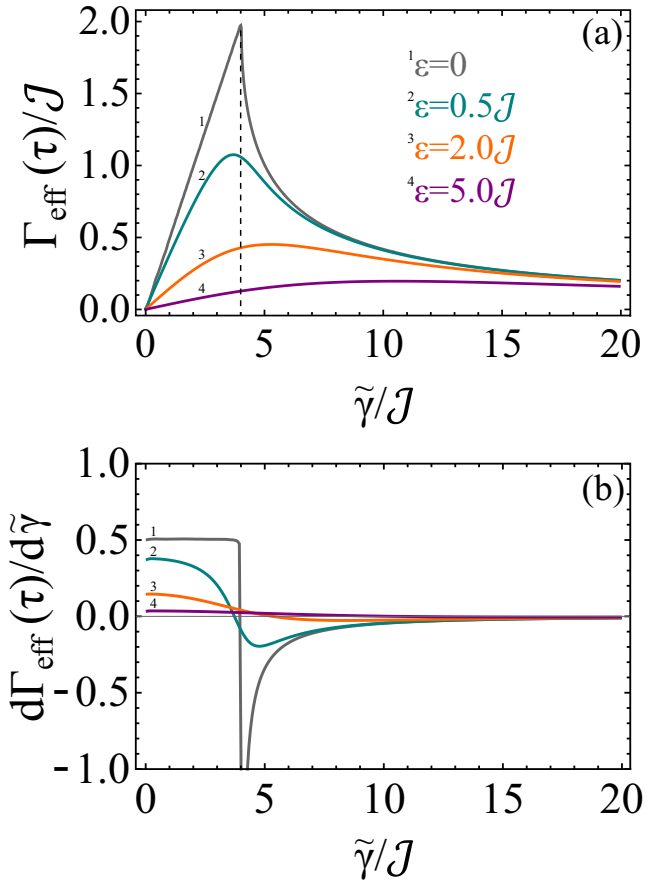

FIG. 4. (a) Effective decay rate for times τ much longer than any other timescale of the system, as a function of $\tilde{\gamma}$, for various qubit energy differences ε. The vertical dashed line at $\tilde{\gamma} = 4\mathcal{J}$ indicates the position of the peak for $\varepsilon = 0$. The gray line (1) denotes $\varepsilon = 0$, the teal line (2) $\varepsilon = 0.5\mathcal{J}$, the orange line (3) $\varepsilon = 2.0\mathcal{J}$, and the purple line (4) $\varepsilon = 5.0\mathcal{J}$. (b) Derivative of the effective decay rate for times τ much longer than any other timescale of the system, with respect to $\tilde{\gamma}$, as a function of $\tilde{\gamma}$. The parameters are the same as those in (a).

The sharpness of the peak can be easily identified trough discontinuities of the first derivative of the effective decay rate with respect to $\tilde{\gamma}$ as in Fig. 4(b). Therefore, if the quantity $\Gamma_{\text{eff}}(\tau)$ could be measured as a function of $\tilde{\gamma}$ for τ much larger than any other timescale of the system, it could be argued that by just studying its peak structure, the presence of an EP could be identified. As will become clear, this method appears to be very useful in cases of systems where explicit expressions of effective Hamiltonians do not exist and therefore no diagonalization is possible.

B. Lorentzian environment

In order to obtain the time dependence of the amplitude marked by a tilde $\tilde{c}_1(t)$ for a Lorentzian boundary environment, one needs to calculate the function $R(t)$ via Eq. (7) for a Lorentzian spectral density $J(\omega)$ and find its Laplace transform $B(s)$, necessary for the inversion of the Laplace transform $F_1(s)$. In a recent paper [7], using similar notation, we calculated $B(s)$ for a Lorentzian spectral density distribution with positive peak frequency and negligible extension to negative frequencies and showed that

$$B(s) = \frac{g^2}{s + \frac{\gamma}{2} + i\Delta_c}, \tag{18}$$

where g is the coupling strength constant between the second qubit and the environment, γ is the width of the distribution, and $\Delta_c \equiv \omega_c - \omega'_{eg}$ is the detuning between the peak frequency ω_c of the distribution and the qubit frequency ω'_{eg} of the second qubit. Substitution of Eq. (18) into Eq. (9) leads to an expression involving a third-order polynomial with respect to s in the denominator. Although the Laplace inversion can be carried out analytically, the resulting expression of $\tilde{c}_1(t)$ is too lengthy to be insightful.

In contrast to the previous case of a Markovian spectral density, now it is not possible to develop an effective Hamiltonian characterizing the open quantum system by eliminating the reservoir degrees of freedom. This inability is associated with the non-Markovian character of the Lorentzian spectral density, which enables information exchange between the system and the environment within finite times. Therefore, an attempt to find the eigenenergies of the open system as a probe of its exceptional points seems ineffectual. Based, however, on the results of Sec. III A, deduced from the study of the effective decay rate maxima, in comparison to what we know from the spectrum of the non-Hermitian Hamiltonian and its exceptional points, we can track the EPs of the system damped by a Lorentzian reservoir.

In Fig. 5(a) we plot the effective decay rate of the first qubit as a function of the time for $\varepsilon = 0$, $\gamma = 0.5\mathcal{J}$, $\Delta_c = 0$, and $g = \mathcal{J}$. Based on the form of the peaked structure of $\Gamma_{\text{eff}}(\tau)$ as a function of g for τ much larger than any other timescale of the system, we expect an exceptional point at $g = 1.41\mathcal{J}$ [see Fig. 5(d), gray line]. For g smaller than the position of the exceptional point, which we will hereafter denote by g_{EP}, the effective decay rate as a function of the time exhibits sharp peaks indicative of the transfer of populations between the two qubits. Note that, contrary to the Markovian reservoir case, part of the excitation can now be transferred from the open system to the environment and vice versa, within finite times. As g is increased towards the value g_{EP}, the sharp peaks begin to be gradually substituted by smooth oscillations [Fig. 5(b)] up to $g = g_{\text{EP}}$, at which point the $\Gamma_{\text{eff}}(t)$ dynamics exhibits only smooth oscillations, as in Fig. 5(c). Note that for $g \geqslant g_{\text{EP}}$, the system lies in the region where the QZE starts to inhibit the evolution of the second qubit. As a result, as g increases, the population of the second qubit becomes increasingly negligible and the smooth oscillations of the effective decay rate of the first qubit reflect oscillations directly between the latter and the environment.

In Fig. 5(d) we show how the effective decay rate at long times τ behaves as a function of g for various Lorentzian widths and $\varepsilon = 0$. As expected, on physical grounds, the decay rate is overall increased as γ increases. At the same time the sharp peak of the curve, which indicates the position of the exceptional point, moves towards larger g. The dependence between the position of the exceptional point g_{EP} and the Lorentzian width γ is depicted in Fig. 5(e). At the same time the maximum of the curve is also affected by the value of

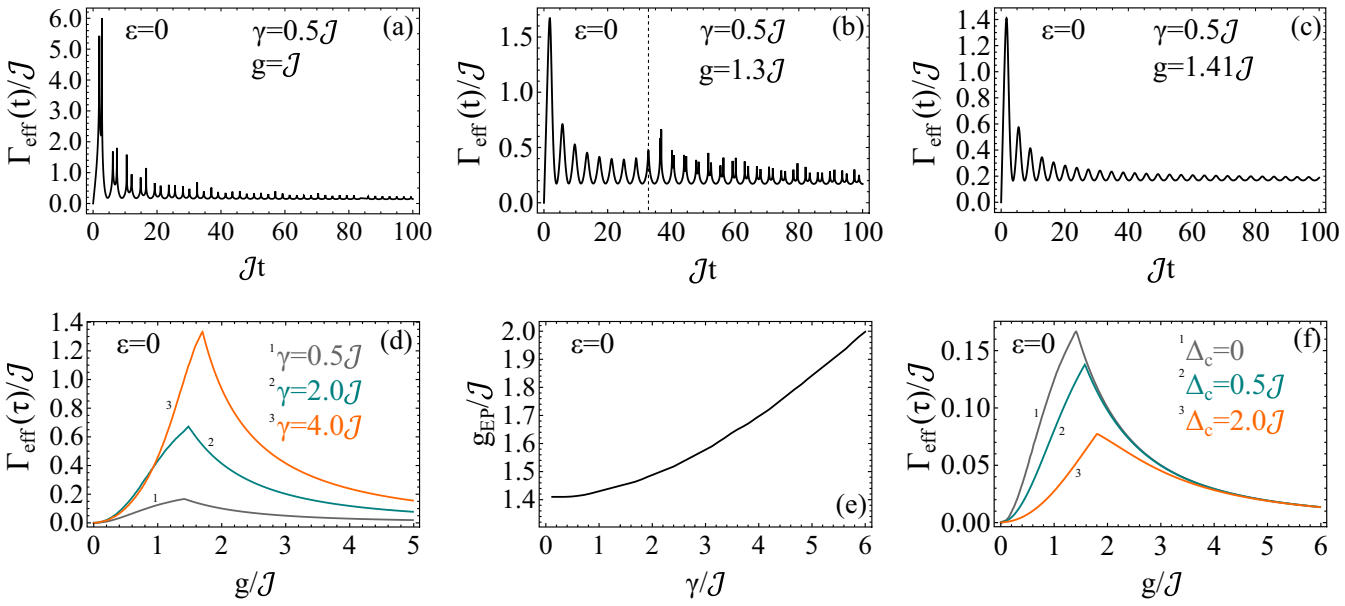

FIG. 5. (a) Time dynamics of the effective decay rate for $\varepsilon = 0$ (identical qubits) and a Lorentzian boundary environment with the parameters $\gamma = 0.5\mathcal{J}$, $g = \mathcal{J}$, and $\Delta_c = 0$. (b) Same as in (a) but for $g = 1.3\mathcal{J}$. The vertical dashed line indicates the time up to which the decay rate oscillations are smooth. (c) Same as in (a) but for $g = 1.41\mathcal{J}$. (d) Effective decay rate for times τ much longer than any other timescale of the system, as a function of g, for various Lorentzian widths γ, $\varepsilon = 0$, and $\Delta_c = 0$. The gray line (1) denotes $\gamma = 0.5\mathcal{J}$, the teal line (2) $\gamma = 2\mathcal{J}$, and the orange line (3) $\gamma = 4\mathcal{J}$. (e) Location of the exceptional point $g_{\rm EP}$ as a function of γ for $\varepsilon = 0$ and $\Delta_c = 0$. (f) Effective decay rate for times τ much longer than any other timescale of the system, as a function of g, for various values of the detuning Δ_c between the Lorentzian peak and the qubit frequency of the second qubit. The parameters used are $\epsilon = 0$ and $\gamma = 0.5\mathcal{J}$. The gray line (1) denotes $\Delta_c = 0$, the teal line (2) $\Delta_c = 0.5\mathcal{J}$, and the orange line (3) $\Delta_c = 2.0\mathcal{J}$.

detuning between the Lorentzian peak and the qubit frequency of the second qubit [Fig. 5(f)]. In view of the above results, we can confidently argue that the positions of the exceptional points in the case of a Lorentzian reservoir show great sensitivity to the values of the Lorentzian parameters γ and Δ_c.

For the results of Fig. 5 we have assumed that $\varepsilon = 0$, i.e., the two identical qubits. In Fig. 6 we examine the effects of a nonzero energy difference between the two qubits on the QZE onset for Lorentzian reservoirs. In Fig. 6(a) we plot the effective decay rate at long times τ as a function of the qubit-environment coupling strength g for various values of ε. As ε is increased, the position of the maximum of the curve tends towards larger coupling strengths, as was the case for a Markovian-damped open system (see Fig. 4). There are however two striking differences. First, in the Markovian case the value of ε affected significantly the width of the effective decay curve, whereas for Lorentzian reservoirs, the increase of ε results roughly in a displacement of the curve towards larger g. Second and most important, in the Markovian case, for any value of ε, the effective decay rate exhibits a smooth maximum, except for the case $\varepsilon = 0$, where the peak is sharp [see the derivative in Fig. 4(b)] and is marked by the presence of an exceptional point. On the other hand, for a Lorentzian reservoir, the peak of the effective decay rate is sharp for any value of ε. This result can be verified upon inspection of the discontinuities of the effective decay rate derivative with respect to g as a function of g for various values of ε [Fig. 6(b)]. Therefore, the maximum points of the effective de-

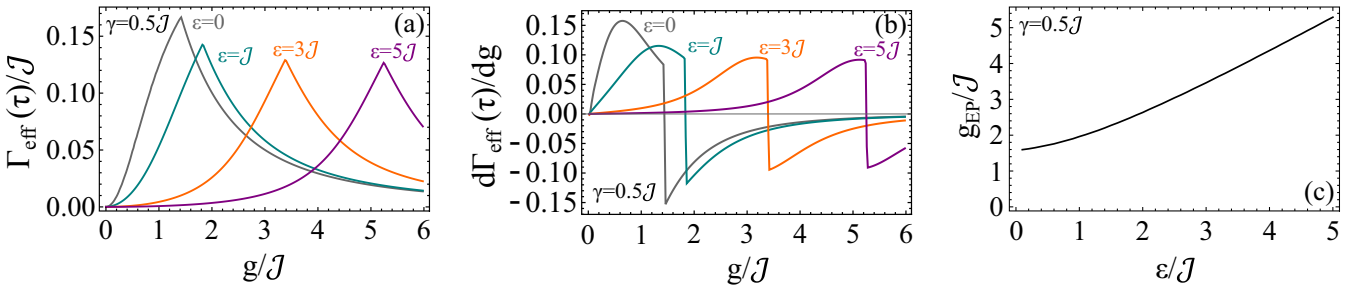

FIG. 6. (a) Effective decay rate for times τ much longer than any other timescale of the system, as a function of g, for various energy differences ε between the two qubits, $\gamma = 0.5\mathcal{J}$, and $\Delta_c = 0$ (Lorentzian boundary reservoir). The gray line denotes $\varepsilon = 0$, the teal line $\varepsilon = \mathcal{J}$, the orange line $\varepsilon = 3\mathcal{J}$, and the purple line $\varepsilon = 5\mathcal{J}$. (b) Derivative of the effective decay rate for times τ much longer than any other timescale of the system, with respect to g, as a function of g, for various ε. The values of the parameters are the same as in (a). (c) Location of the exceptional point as a function of ε for $\gamma = 0.5\mathcal{J}$ and $\Delta_c = 0$.

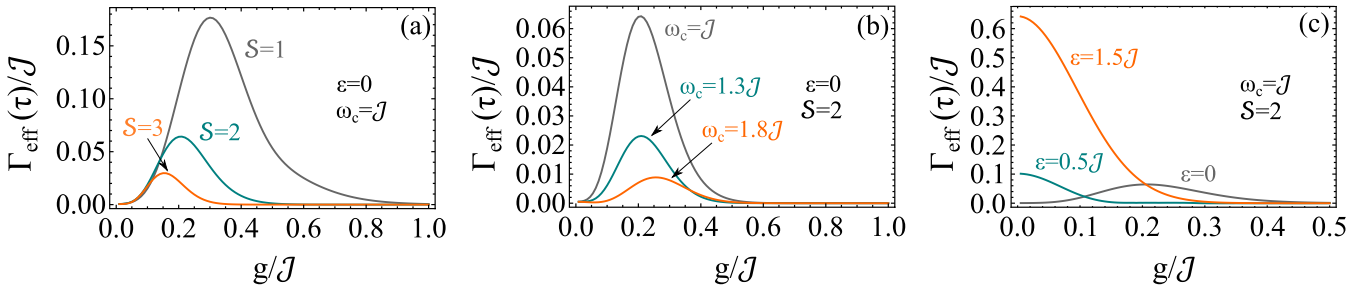

FIG. 7. (a) Effective decay rate for times τ much longer than any other timescale of the system, as a function of g, for various Ohmic parameters $\mathcal{S}$, $\omega_c = \mathcal{J}$, $\varepsilon = 0$, and $\omega_{eg} = 6\mathcal{J}$. The gray line denotes $\mathcal{S} = 1$, the teal line $\mathcal{S} = 2$, and the orange line $\mathcal{S} = 3$. (b) Effective decay rate for times τ much longer than other timescales of the system, as a function of g, for various cutoff frequencies ω_c, $\mathcal{S} = 2$, $\varepsilon = 0$, and $\omega_{eg} = 6\mathcal{J}$. The gray line denotes $\omega_c = \mathcal{J}$, the teal line $\omega_c = 1.3\mathcal{J}$, and the orange line $\omega_c = 1.8\mathcal{J}$. (c) Effective decay rate for times τ much longer than other timescales of the system, as a function of g, for various energy differences ε between the two qubits, $\mathcal{S} = 2$, $\omega_c = \mathcal{J}$, and $\omega_{eg} = 6\mathcal{J}$. The gray line denotes $\varepsilon = 0$, the teal line $\varepsilon = 0.5\mathcal{J}$, and the orange line $\varepsilon = 1.5\mathcal{J}$.

cay rate mark the existence of exceptional points for any value of ε in the case of a Lorentzian reservoir. The dependence of the positions of such points as a function of ε is depicted in Fig. 6(c).

C. Ohmic environment

In this section we examine the case of a reservoir characterized by an Ohmic spectral density [56,57]. In that case $J(\omega)$ is given by

$$J(\omega) = \mathcal{N} g^2 \omega_c \left(\frac{\omega}{\omega_c}\right)^{\mathcal{S}} \exp\left(-\frac{\omega}{\omega_c}\right), \tag{19}$$

where ω_c is the so-called Ohmic cutoff frequency and $\mathcal{S}$ the Ohmic parameter, characterizing whether the spectrum of the reservoir is sub-Ohmic ($\mathcal{S} < 1$), Ohmic ($\mathcal{S} = 1$), or super-Ohmic ($\mathcal{S} > 1$). In addition, $\mathcal{N}$ is a normalization constant given by the relation $\mathcal{N} = \frac{1}{(\omega_c)^2 \Gamma(1+\mathcal{S})}$, where $\Gamma(z)$ is the Gamma function.

The corresponding function $B(s)$, which is the Laplace transform of the function $R(t)$ given by Eq. (7), has been calculated in previous work for Ohmic spectral densities [7] and was found to be given by

$$B(s) = -g^2 \frac{i^{1-\mathcal{S}}}{\omega_c} e^{-iK(s)} [K(s)]^{\mathcal{S}} \Gamma(-\mathcal{S}, -iK(s)), \tag{20}$$

where $K(s) \equiv (s - i\omega_{eg})/\omega_c$ and $\Gamma(a, z)$ is the incomplete Gamma function. Substitution of Eq. (20) into Eq. (9) leads to an expression for $F_1(s)$ whose inverse Laplace transform can be calculated numerically to yield the time dependence of $\tilde{c}_1(t)$.

In Fig. 7 we plot the effective decay rate of the first qubit at long times τ, as a function of the qubit-reservoir coupling strength g, for various combinations of the remaining parameters. In Fig. 7(a) we examine the effects of varying the Ohmic parameter $\mathcal{S}$ on the behavior of the effective decay rate profile in the case of identical qubits ($\varepsilon = 0$). The effective decay rate is now found to exhibit a peak for any value of $\mathcal{S}$. However, it is not sharp, i.e., the first derivative of the effective decay rate with respect to g, as a function of g, does not exhibit a discontinuity at the position of the peak. Although this suggests that the QZE occurs for any value of $\mathcal{S}$, it is not accompanied by the presence of an EP. The onset of the QZE (position of the maximum) decreases as the Ohmic parameter is increased. At the same time, the overall decay rate decreases as $\mathcal{S}$ is increased, which can be interpreted in terms of the form of the Ohmic spectral density distribution as a function of $\mathcal{S}$. In particular, for fixed ω_c and increasing $\mathcal{S}$, the distribution tends to flatten, causing more dominant modes of the distribution to be off-resonance from the qubit frequency, thus damping the system less efficiently. The difference between the effects of the Ohmic and Lorentzian distributions can be attributed to the fact that the flattening of the distribution and the position of its peak is controlled by different parameters in the two cases. For the Lorentzian, they are γ and Δ_c (for fixed ω_{eg}), respectively, whereas for an Ohmic distribution both of them depend on the Ohmic parameters $\mathcal{S}$ and ω_c. Note that the Ohmic distribution exhibits a peak at the frequency $\mathcal{S}\omega_c$.

In Fig. 7(b) we keep the Ohmic parameter fixed to the value $\mathcal{S} = 2$ and examine the behavior of the effective decay rate as a function of the cutoff frequency of the distribution. The results indicate that the onset of the QZE occurs for larger qubit-environment couplings g, as the cutoff frequency is increased. Again, the effective decay rate shows no evidence of the presence of EPs, for any combination of the Ohmic parameters. The values of the decay rate decrease as ω_c is increased, owing to the flattening of the distribution for fixed $\mathcal{S}$ and increasing ω_c, along the lines of interpretation in the preceding paragraph.

Finally, in Fig. 7(c) we examine the behavior of the effective decay rate for various values of the energy difference between the two qubits. Interestingly, contrary to the case of identical qubits, when $\varepsilon \neq 0$, the effective decay rate is maximum at $g = 0$ and decreases as g is increased. This result indicates that the system lies in the QZE regime for any value of g.

IV. CONCLUSION

We have investigated a method of tracking EPs in a non-Markovian open quantum system, for which a closed-form expression of the effective Hamiltonian describing the open system may not exist. In that case, the EPs of the system cannot be found by following the usual procedure of Hamiltonian diagonalization, as would have been the case for a quantum system damped by one or more Markovian reser-

voirs. Although our theory in this paper deals with the simple case of two nonidentical qubits, one of which interacts with a reservoir of arbitrary spectral density, our method is readily generalizable to any number of qubits and reservoirs.

The method is based upon studying the behavior of the effective decay rate of the first qubit as a function of the coupling between the environment and the second qubit. We first studied the case of Markovian damping where the system is diagonalizable and we compared the effective decay rate analysis with the analysis in terms of the eigenvalues of the open system. The results indicated that although a peak of the effective decay rate term is always associated with the onset of the QZE, if the peak is sharp (i.e., if the first derivative of the effective decay rate with respect to g as a function of g exhibits a discontinuity), the system has an EP at the position of the peak.

We further examined the cases of reservoirs characterized by Lorentzian as well as Ohmic spectral densities. For Lorentzians, we have shown that the system will always have a single EP, for any combination of the parameters of the spectral density, i.e., its width and the detuning of its peak from the qubit frequency. The position of the EP (g_{EP}) has been found to shift towards higher values as γ increases for fixed Δ_c or as Δ_c increases for fixed γ. Interestingly, in contrast to the case of Markovian damping where the EP exists only for identical qubits ($\varepsilon = 0$), for a Lorentzian reservoir, an EP is always present irrespective of the value of ε. On the other hand, for reservoirs with an Ohmic spectral density, our results indicate that, although the system has a critical coupling marking the onset of the QZE (peak of the effective decay rate curve), this onset is not accompanied by the presence of an EP (i.e., the peak is not sharp), for any combination of the Ohmic parameters. The position of this onset was found to move towards smaller values of g, as the Ohmic parameter $\mathcal{S}$ is increased or as the Ohmic cutoff frequency ω_c is decreased. For $\varepsilon \neq 0$ the effective decay rate is maximum at $g = 0$, decreasing monotonically as g is increased. Therefore, in the case of two nonidentical qubits and an Ohmic environment, the system will lie within the QZE regime, for any value of g.

We believe that the significance of our results rests upon the synthesis of exceptional points in the presence of non-Markovian dissipation. Although both aspects represent problems of extensive current research activity, their combined effect in the same quantum system has hardly been explored. However, the dynamics of open quantum systems associated with the presence of EPs or/and the regions of the onset of the QZE beyond Markovianity is of great significance in a plethora of realistic situations, many of practical interest. Our method can account for any form of the boundary environment's spectral density and can easily be generalized to open quantum systems consisting of qubits and environments interacting in more complex arrangements. The drastic differences in the effective decay rate of the first qubit as a function of g, between a boundary environment of Lorentzian spectral density from that of Ohmic, raises the following profound question: What are the necessary conditions that an arbitrary spectral density should satisfy to result in the existence of EPs for certain regions of parameters? Whether these conditions are related to symmetries of the spectral density profile or other features remains to be examined in future work, with possibly quite impactful implications. Nevertheless, the contrast between the effect of a Lorentzian and an Ohmic spectral density on the EPs in our system illustrates the resistance of non-Markovian distributions to general classifications.

ACKNOWLEDGMENTS

G.M. would like to acknowledge the Hellenic Foundation for Research and Innovation (HFRI) for financially supporting this work under the 3rd Call for HFRI Ph.D. Fellowships (Fellowship No. 5525). We are also grateful to T. Ilias for useful discussions concerning this work.

[1] I. de Vega and D. Alonso, Rev. Mod. Phys. **89**, 015001 (2017).
[2] H.-P. Breuer, E.-M. Laine, J. Piilo, and B. Vacchini, Rev. Mod. Phys. **88**, 021002 (2016).
[3] C. M. Bender, Rep. Prog. Phys. **70**, 947 (2007).
[4] W. D. Heiss, J. Phys. A: Math. Theor. **45**, 444016 (2012).
[5] W. M. Itano, D. J. Heinzen, J. J. Bollinger, and D. J. Wineland, Phys. Rev. A **41**, 2295 (1990).
[6] K. Koshino and A. Shimizu, Phys. Rep. **412**, 191 (2005).
[7] G. Mouloudakis, T. Ilias, and P. Lambropoulos, Phys. Rev. A **105**, 012429 (2022).
[8] See, for example, H. P. Breuer and F. Petruccione, *The Theory of Open Quantum Systems* (Oxford University Press, Oxford, 2002).
[9] G. Mouloudakis and P. Lambropoulos, Quantum Inf. Process. **20**, 331 (2021).
[10] S. He, L.-W. Duan, C. Wang, and Q.-H. Chen, Phys. Rev. A **99**, 052101 (2019).
[11] J. Peise, B. Lucke, L. Pezze, F. Deuretzbacher, W. Ertmer, J. Arlt, A. Smerzi, L. Santos, and C. Klempt, Nat. Commun. **6**, 6811 (2015).
[12] Y. Li, X. Chen, and M. P. A. Fisher, Phys. Rev. B **98**, 205136 (2018).
[13] M. C. Fischer, B. Gutierrez-Medina, and M. G. Raizen, Phys. Rev. Lett. **87**, 040402 (2001).
[14] W. Zheng, D. Z. Xu, X. Peng, X. Zhou, J. Du, and C. P. Sun, Phys. Rev. A **87**, 032112 (2013).
[15] F. Schäfer, I. Herrera, S. Cherukattil, C. Lovecchio, F. S. Cataliotti, F. Caruso, and A. Smerzi, Nat. Commun. **5**, 3194 (2014).
[16] K. Kakuyanagi, T. Baba, Y. Matsuzaki, H. Nakano, S. Saito, and K. Semba, New J. Phys. **17**, 063035 (2015).
[17] P. M. Harrington, J. T. Monroe, and K. W. Murch, Phys. Rev. Lett. **118**, 240401 (2017).
[18] E. W. Streed, J. Mun, M. Boyd, G. K. Campbell, P. Medley, W. Ketterle, and D. E. Pritchard, Phys. Rev. Lett. **97**, 260402 (2006).
[19] S. Maniscalco, F. Francica, R. L. Zaffino, N. Lo Gullo and F. Plastina, Phys. Rev. Lett. **100**, 090503 (2008).
[20] S.-C. Wang, Y. Li, X.-B. Wang, and L. C. Kwek, Phys. Rev. Lett. **110**, 100505 (2013).

[21] A. Nourmandipour, M. K. Tavassoly, and M. Rafiee, Phys. Rev. A **93**, 022327 (2016).
[22] A. Nourmandipour, M. K. Tavassoly, and M. A. Bolorizadeh, J. Opt. Soc. Am. B **33**, 1723 (2016).
[23] P. Facchi and S. Pascazio, Phys. Rev. Lett. **89**, 080401 (2002).
[24] P. Facchi and S. Pascazio, J. Phys. A: Math. Theor. **41**, 493001 (2008).
[25] K. Koshino and A. Shimizu, Phys. Rev. A **67**, 042101 (2003).
[26] M. Hotta and M. Morikawa, Phys. Rev. A **69**, 052114 (2004).
[27] M. G. Makris and P. Lambropoulos, Phys. Rev. A **70**, 044101 (2004).
[28] S. Wallentowitz and P. E. Toschek, Phys. Rev. A **72**, 046101 (2005).
[29] M. Ozawa, Phys. Lett. A **356**, 411 (2006).
[30] S. Wallentowitz and P. E. Toschek, Phys. Lett. A **367**, 420 (2007).
[31] L. S. Schulman, Phys. Rev. A **57**, 1509 (1998).
[32] B. Nagels, L. J. F. Hermans, and P. L. Chapovsky, Phys. Rev. Lett. **79**, 3097 (1997).
[33] K. Mølhave and M. Drewsen, Phys. Lett. A **268**, 45 (2000).
[34] T. Nakanishi, K. Yamane, and M. Kitano, Phys. Rev. A **65**, 013404 (2001).
[35] W. Wu and H.-Q. Lin, Phys. Rev. A **95**, 042132 (2017).
[36] J. Li, T. Wang, L. Luo, S. Vemuri, and Y. N. Joglekar, arXiv:2004.01364.
[37] P. Kumar, A. Romito, and K. Snizhko, Phys. Rev. Res. **2**, 043420 (2020).
[38] T. Chen, W. Gou, D. Xie, T. Xiao, W. Yi, J. Jing, and B. Yan, npj Quantum Inf. **7**, 78 (2021).
[39] M. Naghiloo, M. Abbasi, Y. N. Joglekar, and K. W. Murch, Nat. Phys. **15**, 1232 (2019).
[40] B. Dora, D. Sticlet, and C. P. Moca, Phys. Rev. Lett. **128**, 146804 (2022).
[41] R. El-Ganainy, K. G. Makris, M. Khajavikhan, Z. H. Musslimani, S. Rotter, and D. N. Christodoulides, Nat. Phys. **14**, 11 (2018).
[42] C. E. Rüter, K. G. Makris, R. El-Ganainy, D. N. Christodoulides, M. Segev, and D. Kip, Nat. Phys. **6**, 192 (2010).
[43] M.-A. Miri and A. Alu, Science **363**, eaar7709 (2019).
[44] S. K. Ozdemir, S. Rotter, F. Nori, and L. Yang, Nat. Mater. **18**, 783 (2019).
[45] S. Garmon and G. Ordonez, J. Math. Phys. **58**, 062101 (2017).
[46] S. Garmon, T. Sawada, K. Noba, and G. Ordonez, J. Phys.: Conf. Ser. **2038**, 012011 (2021).
[47] K. Snizhko, P. Kumar, and A. Romito, Phys. Rev. Res. **2**, 033512 (2020).
[48] W. Chen, S. K. Ozdemir, G. Zhao, J. Wiersig, and L. Yang, Nature (London) **548**, 192 (2017).
[49] M. I. N. Rosa, M. Mazzotti, and M. Ruzzene, J. Mech. Phys. Solids **149**, 104325 (2021).
[50] X.-G. Wang, G.-H. Guo, and J. Berakdar, Phys. Rev. Appl. **15**, 034050 (2021).
[51] C. Zeng, Y. Sun, G. Li, Y. Li, H. Jiang, Y. Yang, and H. Chen, Opt. Express **27**, 27562 (2019).
[52] H. Hodaei, A. U. Hassan, S. Wittek, H. Garcia-Gracia, R. El-Ganainy, D. N. Christodoulides, and M. Khajavikhan, Nature (London) **548**, 187 (2017).
[53] P. Lambropoulos and D. Petrosyan, *Fundamentals of Quantum Optics and Quantum Information* (Springer, Berlin, 2007).
[54] D. F. Walls and G. J. Milburn, *Quantum Optics* (Springer, Berlin, 2008).
[55] J. J. Sakurai, *Advanced Quantum Mechanics* (Addison-Wesley, Reading, 1967).
[56] A. J. Leggett, S. Chakravarty, A. T. Dorsey, Matthew P. A. Fisher, A. Garg, and W. Zwerger, Rev. Mod. Phys. **59**, 1 (1987); **67**, 725 (1995).
[57] U. Weiss, *Quantum Dissipative Systems* (World Scientific, Singapore, 2001).